31st International Conference Nuclear Energy for New Europe
NENE 2022, September 12-15, Portorož, Slovenia

# On the Calculation of Adjoint Neutron Flux in a Typical PWR for the Determination of the Neutron Flux Redistribution Factors

**Tanja Goričanec, Luka Snoj, Marjan Kromar**
Reactor Physics Department, Jožef Stefan Institute
Jamova cesta 39
SI-1000 Ljubljana
tanja.goricanec@ijs.si, luka.snoj@ijs.si, marjan.kromar@ijs.si

## ABSTRACT

Deterministic (DENOVO) and stochastic (MCNP) approaches are used for calculating adjoint neutron flux distribution in a typical pressurized water reactor. The calculated adjoint neutron flux distributions were used to calculate neutron flux redistribution factors, which are used in analysis of control rod worth measurements with the rod insertion method. A sensitivity analysis of the geometry representations of the adjoint and forward distributions confirmed that the geometry description (voxel size) has a noticeable effect on the calculated neutron flux redistribution factors. To verify the results, a comparison was made with the calculated neutron flux redistribution factors obtained by calculating the direct ex-core detector response with the MCNP ex-core model. A pin-wise description of the adjoint neutron flux calculated with ADVANTG (DENOVO) code in 24 axial layers gave the best agreement with a deviation from the reference results of ~ 2 %. Presented analysis indicates, that stochastic method, applied in this paper might not be applicable for adjoint neutron flux distribution calculation.

## 1 INTRODUCTION

For safe operation of the nuclear reactor it is important to accurately know the differential and integral control rod reactivity worth. The control rod reactivity worth can be measured using various techniques (i.e. boron dilution, rod swap, rod drop, etc.). A newer method, called the rod insertion method [1] was developed at the Jožef Stefan Institute (JSI) Reactor Physics Department. It relies on the analysis of the reactor signal, which is recorded during continuous insertion of the control rod bank. Its major advantage is high execution speed (approximately 15 minutes per control rod bank) in contrast to the most widely used boron dilution method, which takes about 4 hours. In a typical nuclear power plant, the differential and integral reactivity worth of the control rod are measured by using the ex-core neutron detectors. As a typical PWR, the Krško NPP was chosen. It is a Westinghouse design plant and has a two loop pressurized water reactor. Currently, the thermal rating is 1994 MWt with 727 MWe gross electric production. The core is composed out of 121 fuel assemblies (see Figure 1). In the reactor core are 33 rod cluster control assemblies distributed as presented in Figure 1. The ex-core uncompensated ionization chambers, as power range detector, monitor neutron flux, during normal reactor operation at power and are also used during rod insertion method. The ex-core detectors are placed in wells, which are located on the cavity wall. Power range detectors are positioned in four equally spaced locations around the core. There are 4 power range channels with 2 vertical detectors per channel.

The rod insertion method is a dynamic method and to obtain realistic control rod worth two types of corrections need to be applied: dynamic-to-static conversion factor [2] and neutron flux redistribution factors (evaluated in this paper). During the insertion of the control rod bank, the spatial distribution of the neutron population in the core is significantly changed. Since the detector measures the local neutron flux at the location outside the core, neutron flux redistribution factors should be applied to obtain a realistic control rod worth. Neutron flux redistribution factors currently used in the NPP Krško have been determined with a single adjoint flux distribution calculation for the first operational cycle [3]. The calculation was performed using 2D deterministic code DOT [4]. In aim to improve the neutron flux redistribution factor calculation with Monte Carlo method and full 3D calculation, a detailed core and ex-core model of a typical pressurized water reactor (PWR) nuclear power plant (NPP) [5], [6] was developed for use in the Monte Carlo neutron transport code MCNP [7]. The ex-core neutron detector response can be determined directly or indirectly by multiplying adjoint neutron flux and fission rate distributions [8]. This work focuses on the evaluation of neutron flux redistribution factors using adjoint neutron flux distributions.

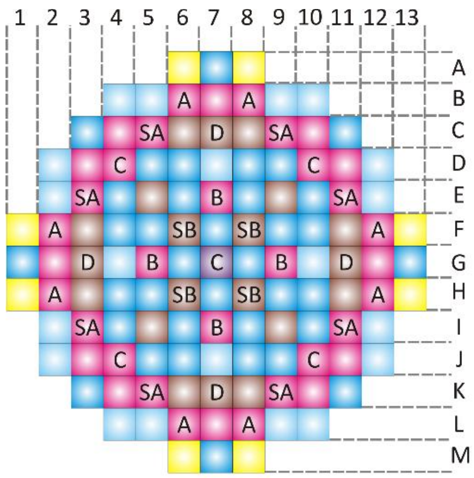

Figure 1: A typical NPP Krško core configuration with marked control rod cluster positions.

## 2 COMPUTATIONAL MODEL

A computational model of the containment building, reactor pressure vessel, reactor core and ex-core detectors, used for presented calculations, was developed using Monte Carlo neutron transport code MCNP6.1.1. [1] with ENDF/B-VIII.0 nuclear data library [9]. Explicitly modelled ex-core detectors with the updated surrounding concrete shape used in calculations are presented in right hand side figure in Figure 2.

The hybrid code ADVANTG [10] used to generate weight windows to speed up neutron transport outside the reactor core, cannot be used for eigenvalue problems. To use ADVANTG code, the core criticality calculation had to be translated to a fixed source problem. Different geometries and prompt fission neutron spectra for fixed source description were compared in previous research [10], where the need for describing pin-wise neutron source together with prompt fission neutron spectra calculated from weighting prompt neutron fission spectra of important isotopes based on calculated reaction rates was identified. Fixed neutron source used for ex-core calculations presented in this paper was described with cylinders on fuel pin scale in 24 equally spaced axial layers. For calculations presented in this paper, fixed neutron source represented hot zero power (HZP) core state for a typical 18 month fuel cycle of the Krško NPP ($28^{th}$ fuel cycle). Calculations were performed for full reactor power of 1994 MW. A detailed MCNP core model used to calculate fixed neutron source was previously verified and validated by comparison to the CORD-2 results and in-core measurements [5].

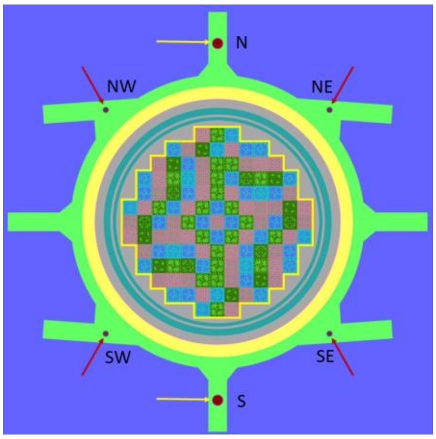

Figure 2: Schematic view of the MCNP ex-core model with marked power range detector locations with red arrows.

## 3 ADJOINT NEUTRON FLUX DISTRIBUTION CALCULATION

The response ($R$) for a detector with response function ($\sigma_d$) can be expressed as:

$$R = \int dp\sigma_d(p)\psi(p), \tag{1}$$

where $p$ refers to independent variables of the particle phase space ($\vec{r}$, $E$, $\hat{\Omega}$), and $\psi$ is the angular neutron flux obtained by solving the forward transport equation [8]. To derive a formulation for the detector response in terms of adjoint function, the relation between the forward and adjoint transport operator must be taken into account:

$$\langle\psi^\dagger, \boldsymbol{H}\psi\rangle = \langle\psi, \boldsymbol{H}^\dagger\psi^\dagger\rangle, \tag{2}$$

where $\psi$ is angular flux, $H$ the transport operator, and $\psi^\dagger$ and $H^\dagger$ their adjoint counterparts. The forward and adjoint transport equation can also be written as:

$$H\psi = q, \qquad H^\dagger\psi^\dagger = q^\dagger, \qquad \langle\psi q^\dagger\rangle = \langle\psi^\dagger q\rangle. \tag{3}$$

Now, if we set:

$$q^\dagger = \sigma_d, \tag{4}$$

then we obtain a new formulation for the detector response ($R$) as [7]:

$$R = \langle\psi^\dagger q\rangle = \int dpq(p)\psi^\dagger(p). \tag{5}$$

It can be concluded, that the detector response corresponds to the integral of the adjoint weighted source distribution. The neutron source distribution can be approximated with the power distribution and the detector response can be approximated with the multiplication of forward and adjoint angular flux distribution as:

$$q = \chi\int dp\nu\Sigma_f(p)\psi(p), \tag{6}$$

$$R = \chi \int dp \nu \Sigma_f(p) \psi(p) \psi^{\dagger}(p), \quad (7)$$

where $\chi$ is the fission neutron spectra, $\nu$ the average number of neutrons produced per fission event and $\Sigma_f$ macroscopic fission cross section.

## 4 RESULTS

The reactor core power distributions were determined using a detailed MCNP model of the reactor core, while the adjoint neutron flux distributions were calculated in two ways. First, the MCNP ex-core model was used to determine the source coordinates of neutrons contributing to the detector response, which can be considered an approximate representation of the adjoint neutron flux. Second, distributions of the adjoint neutron flux determined using the ADVANTG (DENOVO) code [10] were used. As a reference a direct method of calculating the ex-core detector response and its deviation with control rods movement using MCNP ex-core model was used. The reference (direct) method for calculating ex-core detector response was described in detail in previous research [6].

### 4.1 Adjoint neutron flux distribution from ADVANTG

The hybrid code ADVANTG is mainly used to generate weight windows to speed up neutron transport. To calculate weight windows, ADVANTG firstly calculates adjoint neutron flux distribution. For calculations of adjoint neutron flux with ADVANTG presented in this paper, FW-CADIS methodology was used to optimize the response of all power range detectors. Calculations were performed with *bplus* multigroup library with 47 neutron energy groups [10]. For other options, default values were used. In left hand-side figure in Figure 3 the adjoint neutron flux distribution calculated on fuel pin scale is presented. In Figure 4 are presented adjoint neutron flux distributions for 2 control rod configurations: all rods out (ARO) and A bank completely inserted (see Figure 1). Adjoint neutron flux distributions presented in Figure 4 are averaged to one core quadrant.

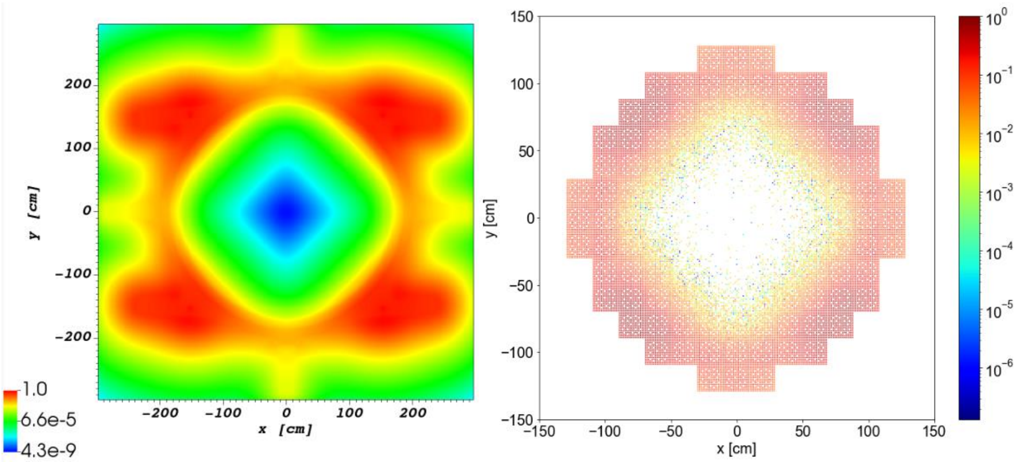


Figure 3: Adjoint neutron flux distribution from ADVANTG (left) and fuel pin contributions from MCNP (right) for ARO at axial slice approximately in the middle of the active fuel height. Results are normalized to the maximum value and presented in colours, ranging from high values in red to low values in blue.

From Figure 3 and Figure 4 it can be observed, that FA closer to the core periphery have higher adjoint neutron flux and therefore contribute more to the detector response. The most important are FAs K-11, L-10 and J-12, which lie on the core diagonal in line with ex-core detectors (see Figure 2). It can be confirmed, that there is only small difference in adjoint neutron flux distribution with different control rod configuration.

| | 7 | 8 | 9 | 10 | 11 | 12 | 13 |
|---|---|---|---|---|---|---|---|
| G | 0.0001 | 0.0002 | 0.0005 | 0.0013 | 0.0035 | 0.0098 | 0.0297 |
| H | 0.0002 | 0.0003 | 0.0008 | 0.0020 | 0.0057 | 0.0160 | 0.0460 |
| I | 0.0004 | 0.0007 | 0.0020 | 0.0059 | 0.0167 | 0.0492 | |
| J | 0.0011 | 0.0021 | 0.0060 | 0.0181 | 0.0539 | 0.1624 | |
| K | 0.0028 | 0.0057 | 0.0170 | 0.0548 | 0.1753 | | |
| L | 0.0077 | 0.0158 | 0.0494 | 0.1671 | | | |
| M | 0.0230 | 0.0467 | | | | | |

| | 7 | 8 | 9 | 10 | 11 | 12 | 13 |
|---|---|---|---|---|---|---|---|
| G | 0.0001 | 0.0002 | 0.0005 | 0.0013 | 0.0035 | 0.0099 | 0.0298 |
| H | 0.0002 | 0.0003 | 0.0008 | 0.0020 | 0.0056 | 0.0158 | 0.0459 |
| I | 0.0004 | 0.0007 | 0.0020 | 0.0059 | 0.0167 | 0.0492 | |
| J | 0.0011 | 0.0021 | 0.0060 | 0.0181 | 0.0539 | 0.1625 | |
| K | 0.0028 | 0.0057 | 0.0170 | 0.0549 | 0.1753 | | |
| L | 0.0077 | 0.0158 | 0.0495 | 0.1672 | | | |
| M | 0.0229 | 0.0468 | | | | | |

Figure 4: Adjoint neutron flux distribution averaged to one core quadrant, calculated with ADVANTG per fuel assembly for ARO (left) and Ain (right). Values are presented in colours, ranging from high values in red to low values in blue.

## 4.2 Adjoint neutron flux from MCNP

The approximation of the adjoint neutron flux distribution was calculated with MCNP by tracking the origin of the particles contributing to the detector response. Calculations were performed with the ex-core MCNP model including explicitly modelled ex-core detectors. Calculations were performed with simulating 2e9 neutron histories and using weight windows generated with the hybrid code ADVANTG. The plotted contributions of fuel pins to ex-core detector response are presented in right hand-side figure in Figure 3. It can be observed that the vast majority of contributions is as expected, from the last two rows of fuel assemblies at the core periphery. Due to the stochastic nature of Monte Carlo calculations, the fuel assemblies closer to the middle of the reactor core have few results and have high statistical uncertainty. In Figure 5 are presented averaged adjoint neutron flux distributions to one core quadrant for 2 control rod configurations (ARO and A bank inserted). It can be observed, that there is significant difference between both configurations, which is in contrast to the observations from ADVANTG method (see Figure 4). In left hand-side figure in Figure 6 are presented relative statistical uncertainties due to the stochastic nature of the MCNP method. In the right-hand side figure in Figure 6 the relative difference between the MCNP and ADVANTG in % is shown.

| | 7 | 8 | 9 | 10 | 11 | 12 | 13 |
|---|---|---|---|---|---|---|---|
| G | 0.0000 | 0.0000 | 0.0001 | 0.0004 | 0.0021 | 0.0147 | 0.0465 |
| H | 0.0000 | 0.0000 | 0.0002 | 0.0007 | 0.0038 | 0.0218 | 0.0523 |
| I | 0.0001 | 0.0002 | 0.0006 | 0.0032 | 0.0152 | 0.0464 | |
| J | 0.0003 | 0.0007 | 0.0031 | 0.0145 | 0.0634 | 0.1389 | |
| K | 0.0020 | 0.0038 | 0.0151 | 0.0632 | 0.1694 | | |
| L | 0.0138 | 0.0217 | 0.0461 | 0.1381 | | | |
| M | 0.0452 | 0.0524 | | | | | |

| | 7 | 8 | 9 | 10 | 11 | 12 | 13 |
|---|---|---|---|---|---|---|---|
| G | 0.0000 | 0.0000 | 0.0001 | 0.0004 | 0.0019 | 0.0102 | 0.0301 |
| H | 0.0000 | 0.0000 | 0.0002 | 0.0009 | 0.0035 | 0.0111 | 0.0327 |
| I | 0.0001 | 0.0002 | 0.0008 | 0.0039 | 0.0167 | 0.0433 | |
| J | 0.0004 | 0.0009 | 0.0039 | 0.0180 | 0.0762 | 0.1573 | |
| K | 0.0018 | 0.0035 | 0.0168 | 0.0761 | 0.2077 | | |
| L | 0.0095 | 0.0111 | 0.0428 | 0.1563 | | | |
| M | 0.0292 | 0.0327 | | | | | |

Figure 5: Adjoint neutron flux distribution averaged to one core quadrant, calculated with MCNP per fuel assembly for ARO (left) and A bank inserted (right). Values are presented in colours, ranging from high values in red to low values in blue.

By comparing results averaged to the one core quadrant between both methods (see Figure 4 and Figure 5) it can be deduced, that the adjoint distribution obtained with MCNP is higher at the core periphery and lower at the centre of the core, compared to the distribution obtained with ADVANTG. This can be explained with stochastic nature of the MCNP method. Because mostly only fuel pins at the edge of the core contribute to the detector response, fuel pins closer to the centre of the core have higher statistical uncertainty, which is also supported with Figure 6. Therefore, it can be concluded that adjoint neutron flux distributions obtain with MCNP, using method described in this paper, are not usable for our purpose. Calculations presented in this paper were performed on computer cluster with 2 processors (Intel Xeon Gold 6148 Processor), each processor with 20 physical cores/ 40 hyper-threading. Calculations ran for ~4.5 days. Correct distributions could be obtained by increasing the number of neutrons simulated, however the number should be increase for at least ×1000, which is in terms of computer time, currently not applicable.

| | 7 | 8 | 9 | 10 | 11 | 12 | 13 |
|---|---|---|---|---|---|---|---|
| G | 23.5 | 10.3 | 5.1 | 2.7 | 1.3 | 0.6 | 0.3 |
| H | 13.4 | 5.1 | 2.3 | 1.3 | 0.6 | 0.3 | 0.2 |
| I | 6.1 | 2.3 | 1.1 | 0.5 | 0.2 | 0.1 | |
| J | 2.6 | 1.2 | 0.5 | 0.2 | 0.1 | 0.1 | |
| K | 1.4 | 0.6 | 0.2 | 0.1 | 0.1 | | |
| L | 0.6 | 0.3 | 0.1 | 0.1 | | | |
| M | 0.4 | 0.2 | | | | | |

| | 7 | 8 | 9 | 10 | 11 | 12 | 13 |
|---|---|---|---|---|---|---|---|
| G | -100.0 | -100.0 | -80.0 | -69.2 | -40.0 | 50.0 | 56.6 |
| H | -100.0 | -100.0 | -75.0 | -65.0 | -33.3 | 36.3 | 13.7 |
| I | -75.0 | -71.4 | -70.0 | -45.8 | -9.0 | -5.7 | |
| J | -72.7 | -66.7 | -48.3 | -19.9 | 17.6 | -14.5 | |
| K | -28.6 | -33.3 | -11.2 | 15.3 | -3.4 | | |
| L | 79.2 | 37.3 | -6.7 | -17.4 | | | |
| M | 96.5 | 12.2 | | | | | |

Figure 6: MCNP Adjoint neutron flux 1 σ relative uncertainty in % for ARO (left) and relative difference between adjoint neutron flux distribution of MCNP and ADVANTG in % (right). Values are presented in colours, ranging from high values in red to low values in blue.

### 4.3 Neutron flux redistribution factors

Neutron flux redistribution factors were determined by comparing the product of adjoint neutron flux and fission rate distribution with bank of interest completely inserted (CRin) and all control rods completely inserted (ARO):

$$f = \frac{\psi^{\dagger}(CRin)FR(CRin)}{\psi^{\dagger}(ARO)FR(ARO)} = \frac{\psi^{\dagger}(CRin)(\psi\sigma_f\overline{\nu})(CRin)}{\psi^{\dagger}(ARO)(\psi\sigma_f\overline{\nu})(ARO)}. \tag{8}$$

Fission rate distributions were calculated with MCNP core model [5]. The calculated neutron flux redistribution factors are presented in Table 1 and Figure 7. Relative statistical uncertainties, originating from the Monte Caro method are < 1 %, however, this does not include uncertainties due to the method or convergence of the results. As the reference, a direct calculations of the difference in detector response using MCNP, without using adjoint neutron flux distribution, are used. In Table 1 and Figure 7 are gathered results obtained from adjoint neutron flux distribution calculated:

- E: per FA in 1 axial layer, ARO adjoint neutron flux,
- F: per FA in 24 axial layers, ARO adjoint neutron flux,
- G: per fuel pin in 24 axial layers, ARO adjoint neutron flux,
- H: per fuel pin in 24 axial layers, individual CR adjoint neutron flux.

When analysing ADVANTG results, the highest deviation in case of Bank A can be observed. With refining geometry voxels to fuel pin level, deviations decreased to below 2 %.

The opposite can be observed with MCNP results, where the lowest deviations are observed on FA scale with 1 axial layer and the highest deviations are for the fuel pin results. This can be explained with the stochastic nature of the method, where uncertainty increases with smaller geometry voxels. The use of presented MCNP method in this paper is not encouraged. It must also be pointed out that for the purpose of this paper the energy dependence of adjoint and forward distributions was not yet taken into account (only total values were used) and will be addressed in future research.

Table 1: Neutron flux redistribution factors using different methods and geometry voxels.

| | Bank A | Bank B | Bank C | Bank D | Bank SA | Bank SB |
|---|---|---|---|---|---|---|
| Reference | 0.907 | 1.143 | 0.946 | 1.024 | 0.841 | 1.130 |
| ADVANTG | | | | | | |
| E | 0.952 | 1.126 | 0.927 | 1.029 | 0.833 | 1.116 |
| $E/Ref - 1$ [%] | 4.91 | -1.50 | -1.99 | 0.46 | -0.94 | -1.26 |
| F | 0.943 | 1.133 | 0.928 | 1.029 | 0.829 | 1.123 |
| $F/Ref - 1$ [%] | 3.97 | -0.81 | -1.92 | 0.46 | -1.44 | -0.64 |
| G | 0.930 | 1.141 | 0.934 | 1.030 | 0.830 | 1.130 |
| $G/Ref - 1$ [%] | 2.52 | -0.16 | -1.20 | 0.56 | -1.28 | -0.02 |
| H | **0.925** | **1.144** | **0.934** | **1.029** | **0.829** | **1.132** |
| $H/Ref - 1$ [%] | **1.96** | **0.16** | **-1.24** | **0.44** | **-1.70** | **0.21** |
| MCNP | | | | | | |
| E | **0.926** | **1.131** | **0.934** | **1.022** | **0.837** | **1.122** |
| $E/Ref - 1$ [%] | **2.06** | **-0.98** | **-1.24** | **-0.28** | **-0.44** | **-0.74** |
| F | 0.931 | 1.127 | 0.936 | 1.027 | 0.843 | 1.119 |
| $F/Ref - 1$ [%] | 2.69 | -1.36 | -1.06 | 0.22 | 0.30 | -1.01 |
| G | 0.930 | 1.130 | 0.936 | 1.029 | 0.842 | 1.120 |
| $G/Ref - 1$ [%] | 2.52 | -1.08 | -1.08 | 0.47 | 0.18 | -0.78 |
| H | 1.006 | 1.118 | 0.942 | 1.040 | 0.856 | 1.109 |
| $H/Ref - 1$ [%] | 10.90 | -2.20 | -0.41 | 1.52 | 1.74 | -1.90 |

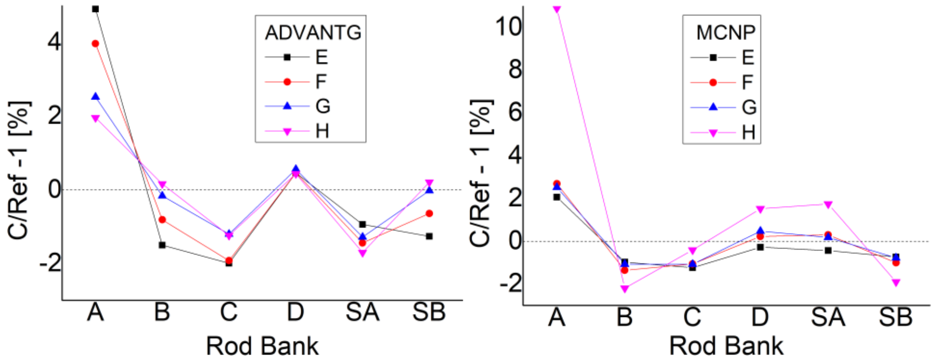


Figure 7: Relative deviation of neutron flux redistribution factors calculated with ADVANTG (left) and MCNP (right) from the reference method (Ref) in %.

## 5 CONCLUSION

The approach for calculating the adjoint neutron flux distribution for typical PWR using stochastic and deterministic methods, in aim to determine neutron flux redistribution factors, is presented. The neutron flux redistribution factors, obtained using different adjoint methods were compared to the results from the reference forward stochastic method. It can be concluded, that the stochastic method, presented in this paper, is not applicable for calculation of adjoint neutron flux distributions. However, the deterministic method, using DENOVO solver in ADVANTG code package, proved to be suitable with the deviations from the reference neutron flux redistribution factors < 2%, for geometry voxels described per fuel pin in 24 axial layers.

## ACKNOWLEDGMENTS

Authors acknowledge the financial support from the Slovenian Research Agency (research core funding No. P2-0073 and project “Development of Computational Tools for the Determination of the Neutron Field in the Containment of the Pressurized Water Reactor” (No. L2-816)).

## REFERENCES

[1] A. Trkov, M. Ravnik, H. Wimmer, B. Glumac, H. Bck, "Application of the rod insertion method for control rod worth measurements in research reactors", Kerntechnik, vol. 60, pp. 255261, 1995.

[2] V. Merljak, M. Kromar and A. Trkov, " Rod insertion method analysis – A methodology update and comparison to boron dilution method”, Annals of Nuclear Engineering, vol. 113, pp. 96-104, 2018.

[3] M. Kromar, et. al, The Nuclear Design and Core Management of the Krško NPP Cycle 26, Jožef Stefan Institute, Ljubljana, Slovenia, IJSDP-11027, 2012.

[4] W. A. Rhoades, DOT IV, Version 4.2: Two Dimensional Discrete Ordinates Radiation Transport Code System, RSIC Code Package CCC-320, ORNL, Oak Ridge, 1979.

[5] T. Goričanec, et al., "Applicability of the Krško Nuclear Power Plant Core Monte Carlo model for the determination of the neutron source term", Nuclear Engineering and Technology, Vol. 53, pp. 3528-3542, 2021.

[6] T. Goričanec, et al., "Predicting Ex-core Detector Response in a PWR with Monte Carlo Neutron Transport Methods", ANIMMA 2019, Portorož, Slovenia

[7] J.T. Goorley, et al., Initial MCNP6 Release Overview - MCNP6 version 1.0, LA-UR-13-22934, 2013.

[8] A. Haghighat, Monte Carlo Methods for Particle Transport, CRC Press, Taylor & Francis Group, 2015.

[9] D. A. Brown, et al., "ENDF/B-VIII.0: The 8th major release of the nuclear reaction data library with CIELO-project cross sections, new standards and thermal scattering data", Nucl. Data Sheets 148(2018)1.

[10] S. W. Mosher, et. al, ADVANTG An Automated Variance Reduction Parameter Generator, August 2015.